

ภาคผนวก

Phase Separation in NR/XSBR Mixed Latices Induced Formation of Micro-porous Films

Wirach Taweepreda^{1,2*}, Thanitaporn Narkkun², Pramuan Tangboriboonrat³

¹*Membrane Science and Technology Research Center, Department of Materials Science and Technology, Faculty of Science, Prince of Songkla University, Hat-Yai, Songkhla 90112, Thailand*

²*NANOTEC Center of Excellence at Prince of Songkla University, Hat-Yai, Songkhla 90112, Thailand*

³*Department of Chemistry, Faculty of Science, Mahidol University, Rama 6 Road, Phyathai, Bangkok 10400, Thailand*

Abstract:

The film formation and surface morphology of natural rubber latex (NRL), carboxylated styrene butadiene rubber (XSBR) latex and their blend were investigated using atomic force microscopy (AFM). For films cast from mixtures of NR and XSBR lattices at 75:25 concentration ratios, XSBR particles were segregated leads to dense clusters of XSBR particles in NR continuous phase due to phase separation. In the dry film at temperature above T_g of XSBR, extensive coalescence of XSBR particles is occurred. On the contrary, addition 75% XSBR in NR/XSBR blend film leads to micro-porous film instead. The nano-scale surface roughness of NR/XSBR film is smaller than film from pure NRL and XSBR latex. However, hydrophilicity of NR/XSBR blend film is increased with increasing XSBR content as well as water and ethanol sorption. The hydrophilic of latex film at film surface was determined using contact angle measurement.

Keywords: latex blend, AFM, membrane, natural rubber, XSBR

*Corresponding author. Tel.: +66-67-785004; Fax: +66-74-446925
E-mail address: wirach.t@psu.ac.th

1. Introduction

Film formation in waterborne coating from an aqueous dispersion of mixed polymer particles has attracted extreme interest in recent decades. [1-4] Film formation mechanism consists of three stages as shown in figure 1. Firstly, the stable dispersion is evaporated results in close packing of particles. Secondly, coalescence of polymer particles leads to a structure without voids, although with the original particles still distinguishable. Finally, the polymer chains diffuse across particle boundaries yields a continuous film with mechanical integrity and the original particles no longer distinguishable. [5] For the latex blending, film properties and morphology are mainly controlled by basic phase behaviors. On one hand, many publications have been revealed to phase separation, since they were blends. [6-11] Phase separation of latex blend is dominated by many factors such as glass transition temperature (T_g) of polymer, annealing temperature, latex composition, drying condition, and substrate. In particular, latex surface morphology and film thickness dependence have received too much attention. [12-16] Latex blend film thickness is decreased with increasing critical temperature or the miscibility of the latex blends due to slow kinetic of phase separation. In contrast, film thickness of polystyrene/poly(vinyl methyl ether) (PS/PVME) blend films was decreased from 1500 nm to 25 nm with decreasing lower critical solution temperature (LCST) from more than 177°C to room temperature.

Figure 1 Film formation mechanism.

Our interest has been in understanding the conditions for controlling film morphology formed from latex blend and the phase separation processes that produce such structure. Blends of natural rubber latex (NRL) with synthetic latex have been reported to be compatible with desirable mechanical properties [17-21]. However, the blending NRL with some polar synthetic latex is difficult task to obtain the desirable properties due to their incompatible nature and hence, they tend to separate out. Furthermore, it is the relative crosslink densities within the individual rubber phase which is of concern and not the extent of crosslinking between the two, although this is also of considerable importance to properties. Thus, better understanding of the vulcanization in a molecular scale is necessary. In this research, the surface structure of a series of latex blends prepared from mixtures of a low T_g NRL and a high T_g carboxylated styrene butadiene copolymer (XSBR) latex dispersion was examined using an atomic force microscope (AFM) because it can provide

high-resolution three-dimensional (3-D) images of the film surface without any sample pretreatment.

2. Experimental

2.1 Materials

High ammonia concentrated natural rubber latex (HA-NRL) was purchased from Chalong Concentrate Latex Industry Co., LTD. Carboxylated styrene butadiene copolymer latex (XSBR) was supplied by Synthomer GmbH. The general properties of both latices are illustrated in table 1. The rubber chemicals for example zinc oxide (ZnO), sulfur (S₈), zinc diethyldithiocarbamate (ZDEC), and vulcanox CPL were all obtained from Lucky four (Bangkok, Thailand) and used without further purification.

Table 1 Physical properties of lattices used

Latex type	T _g (°C)	Particle size (nm)	%TSC	Specific gravity @25°C
HA-NRL	-68	292-1053	61.7	0.92
XSBR	+4	250	50.0	1.02

2.2 Preparation of latex film

NR and XSBR latex were readily mixed together for 10 minutes at an ambient temperature with the following blending ratios: 75:25, 50:50, and 25:75 w/w; based on dry rubber content. For compounding were mixed with chemicals followed Table 2 with mechanical stirred for 24 hours and matured 24 hours at an ambient temperature. The latex films were formed by casting with casting knife on the glass plate with thickness not over than 0.2 mm, approximately. Then, the natural rubber latex films were dried at room temperature and vulcanization was finally at 120°C for 10 minute.

Table 2 Formulation of latex compound.

Compositions	Part per hundred of rubber (phr)				
	1	2	3	4	5
NR latex	100	57	50	25	0
Synthetic latex	0	25	50	75	100
KOH 10% solution	0.5	0.5	0.5	0.5	0.5
K'oleate 10% solution	0.25	0.25	0.25	0.25	0.25
Sulfur 50% dispersion	1.0	1.0	1.0	1.0	1.0
Zinc oxide 50% dispersion	0.5	0.5	0.5	0.5	0.5
ZBDC 50% dispersion	1.0	1.0	1.0	1.0	1.0
Vulcanox CPL50% dispersion	0.75	0.75	0.75	0.75	0.75

2.3 Measurements

2.3.1 Surface characterization of the latex blend films

The AFM measurements (True Non-Contact ModeTM, Park System XE70) were conducted under ambient condition. The silicon nitride cantilever probe vibrates near resonant frequency of piezoelectric modulator passes over a film surface which was placed on pre-cleaned mica substrate, and correlate changes in the cantilever's vibrations to topographical features. The surface roughness average (R_a) and root mean squared (R_q) were calculated from Nanoscope software by using the following equation:

$$R_a = \frac{1}{n} \sum_{j=1}^n |Z_j| \quad (1)$$

$$R_q = \sqrt{\frac{1}{n} \sum_{j=1}^n Z_j^2} \quad (2)$$

Where Z_j is the difference between the height and the mean plane current, and n is number of points.

The friction coefficient of latex blends film surface was measured by using a friction test achine (Plint, TE 75R). The sliding speed and the normal load applied on the rubber surface were kept constant at 0.25 mm/s and 2N, respectively.

2.3.2 Sorption experiments

The membrane was cut into circular shape with 2 cm diameter. The thickness and initial weight of the samples were taken. The increasing weight of sample was investigated every 5 minutes after the sample was soaked in water which kept in bottle by electronic balance. The weighted sample was then immediately replaced into the bottle until the equilibrium was attained. The experimental was also carried out using ethanol. The solvent sorption of the sample (S) was computed using the following equation,

$$S = \frac{Ws - Wd}{Wd} \times 100 \quad (3)$$

Where S is the percentage of solvent sorption, Ws is the weight of sample after soaked in the solvent until the equilibrium was attained and Wd is the initial weight of sample.

3. Results and discussion

The surface morphology from AFM of the NRL film, pouring onto freshly cleaved mica surface and allowing the film to dry slowly at 30°C, showed the roughness and uniformity of the film because of the polydispersity of the NRL particles as shown in figure 2. When such latex is dried, packing of the particles occurs as they come into contact with each other. The surface roughness average (R_a) and root mean squared (R_q) of NRL film were calculated and demonstrated as shown in figure 3 and table 3. The roughness of longitudinal rugged NRL films, compose of aggregates of particles, is smaller than that of vertical axis. On one hand, the monodisperse synthetic latex film, XSBR, arrays of orderly arranged particles with sharp spherical contours as shown in figure 4 and 5. The roughness of XSBR film is slight broader than NRL film. The polydisperse nature of the NRL is clearly revealed. The impurities of NRL, mainly proteins, accumulate in the space between the coalescing particles and form a very tiny exudates spot the entire film surface which are discernible at the early stage of film formation. [22]

Figure 2 AFM images of NRL film on pre-cleaned mica surface at room temperature.

Figure 3 Measurement of NR membrane surface roughness using AFM.

Table 3 Surface roughness values of NRL and XSBR films on mica substrate.

Latex	R_q (nm)		R_a (nm)	
	X-axis	Y-axis	X-axis	Y-axis
NRL	31.7	42.6	24.5	32.5
XSBR	53.1	47.0	42.4	37.3

Figure 4 AFM images of XSBR latex film on pre-cleaned mica surface.

Figure 5 Measurement of XSBR film surface roughness using AFM.

Figure 6 shows the AFM images of XSBR latex film which was dropped onto pre-cleaned mica surface and allowed the film to dry at different temperature above the T_g of XSBR. The latex film drying slowly at 30°C shows particles with sharp spherical contours. The mica surface itself is smooth on the atomic scale. [23] Thus the textures observed in the AFM micrographs are due to features only of the films. The film surface drying at high temperature had no spherical contours. Instead, many indentations were observed on this film surface. The occurrence of these indentation structures is due to the collapse of the latex particles during film formation and degree of crosslinking. Since, XSBR particles are readily crosslink owing to the presence of carboxyl groups. Film obtained from highly crosslinked particles shows highly indented surface. This evidence was supported by NRL film surface as shown in figure 7. Film obtained from NRL compound shows particles with sharp oval contours and indentation structures after vulcanization process at high temperature. During

the film formation at high temperature, “indented” might leaved on the top of individual latex particles within the top surface layer of the film at the same time with vulcanization process.

Figure 6 AFM images of XSBR film drying at:

(A) room temperature (B) 100°C and (C) 120°C.

Figure 7 AFM images of NR latex compound film on mica surface.

Figure 8 show AFM images for each of two different latex blend compositions compared with pure latex. An interesting observation to all blend images is the virtually complete deformation of the soft particles with low T_g of NR. The extent of soft particle coalescence is remarkable. The surface of the blend with high NRL concentration appears smooth and continuous indicating that the soft particles have probably coalesced and melt into the interstitial spaces. For the blend with low NRL concentration, the hard particles of XSBR seem to be held together by a “glue” of deformed soft particles and microvoids in the film is occurred. The presence of microporous in the film is an indication of the inability of the soft polymer to fill completely the spaces between the individual hard particles.

Figure 8 AFM images of drying latex film at room temperature:

(A) NR (B) XSBR 25 : NR 75 (C) XSBR 75 : NR 25 and (D) XSBR.

The vulcanized film surface is completely difference as shown in figure 9. The film surface is smooth with increasing the hard particles concentration. However, the microporous in the blend film with low NRL concentration is exit with diameter around 1 μm depend on degree

of vulcanization and compatibility of NRL and XSBR. According to hard XSBR particle is readily crosslink, not only the presence of carboxyl groups but also the limited double bond in the latex structure. In the presence of ZnO, the XSBR are vulcanized by the formation of salt-like bonds combined with sulfidic bonds and the participation of the carboxyl groups attached to different chains results in the formation of a tridimensional structure. Thus, the vulcanized XSBR film surface has low friction coefficient when compared with NR film as illustrated in figure 10. The coating or mixing of hard particle in NRL surface had been reported that the friction coefficient is reduced. [24,25] The blending of NR with XSBR, hard XSBR particle might be migrated and transferred to the top layer of the latex film and reduces the friction coefficient of the film surface. On one hand, the vulcanized film surface with high content of hard XSBR particle is more hydrophilicity owing to charges surrounding the XSBR particle as indicated by drop shape on latex membrane shown in figure 11.

Figure 9 AFM images of vulcanized latex film at 120°C:

(A) NR (B) XSBR 25 : NR 75 (C) XSBR 75 : NR 25 and (D) XSBR.

Figure 10 Friction coefficient of NR and NR/XSBR blends.

Figure 11 Water drop shape on latex membrane

(A) NR (B) XSBR 25 : NR 75 (C) XSBR 75 : NR 25 and (D) XSBR.

The solvent sorption of the latex blends as shown in figure 12 found that increasing of XSBR composite will increases ethanol sorption. While the water uptake is increased and equal in all composition of XSBR blends due to the high polarity of XSBR. Moreover, the results can be explained in terms of the immiscibility of two latices. The latex film formation is according to the gravity and polarity difference of two latices enhances asymmetric membrane with thermodynamically immiscible. The ethanol sorption depends on the swelling of rubber. The XSBR with high M_c and low cross-linking density will increase the free volume for ethanol uptake.

Figure 12 Water and ethanol sorption of NR and NR/XSBR blends.

Conclusions

The surface of film formed from soft NRL particle shows particles with sharp oval contours owing to their impurity and polydispersity of the NRL particles. The surface morphology and surface roughness were examined using atomic force microscope technique in the Tru Non-Contact ModeTM. The monodisperse XSBR latex form film with circular particle which are discernible at the early stage of film formation. The particles with circular contours on the surface were changed to indentation structure after drying at high temperature because XSBR particles are readily crosslink. As well as the surface structure of vulcanized film from NRL compound. For the film surface of NRL and XSBR blending, hard XSBR particles seem to be held together by a “glue” of deformed soft NRL particles and appear microvoids in the film surface. This microvoids or microporous are also distributed in the vulcanized latex blends film when the hard particle volume fraction exceeds ~ 0.75 even though the film surface is smooth after vulcanization process. The friction coefficient of latex blends films was reduced in the film formed from latex blend dispersions consisting of hard and soft particles when the hard particle volume fraction exceeds ~ 0.5 as well as the hydrophilicity of latex film. This evidence indicates the phase separation and transfer of hard particles to the top surface layer and inability of the soft particles to fill completely the spaces between the individual hard particles.

Acknowledgement

We acknowledge the financial support given by The Thailand Research Fund (TRF)/the Commission on Higher Education (CHE) under MRG project no. 5080206.

References

1. J. Sun, W. W. Gerberich, L. F. Francis, "Transparent, conductive polymer blend coating from latex-based dispersions", *Progress in Organic Coatings*, **59**(2), pp. 115-121, 2007.
2. J.W. Vanderhoff, H.L. Tarkowski, M.C. Jenkins, E.B. Bradford, "Theoretical consideration of the interfacial forces involved in the coalescence of latex particles", *J. Macromol. Chem.*, **1**(2), pp. 361-397, 1966.
3. G.L. Brown, "Formation of films from polymer dispersions", *J. Polym. Sci.*, **22**, pp. 423-434, 1956.
4. D.P. Sheetz, "Formation of films by drying of latex", *J. Appl. Polym. Sci.*, **9**, pp. 3759-3773, 1965.
5. W.A. Henson, D.A. Taber, E.B. Bradford, "Mechanism of film formation of latex paint", *Ind. Eng. Chem.*, **45**(4), pp. 735-739, 1953.
6. A.A. Patel, J. Feng, M.A. Winnik, G.J. Vancso, C.B.D. McBain, "Characterization of latex blend films by atomic force microscopy", *Polymer*, **37**(25), pp. 5577-5582, 1996.
7. J. P. Tomba, X. Ye, F. Li, M. A. Winnik, W. Lau, "Polymer blend latex films: Miscibility and polymer diffusion studied by energy transfer", *Polymer*, **49**(8), pp. 2055-2064, 2008.
8. Y. Chevalier, M. Hidalgo, J.-Y. Cavaillé, B. Cabane, "Small angle neutron scattering studies of composite latex film structure", *Progress in Organic Coatings*, **32**(1-4), pp. 35-41, 1997.
9. J.M. Stubbs, Y.G. Durant, D.C. Sundberg, "Polymer phase separation in composite latex particles. 1. Considerations for the nucleation and growth mechanism", *Comptes Rendus Chimie*, **6**, pp. 1217-1232, 2003.
10. J.M. Stubbs, D.C. Sundberg, "The dynamics of morphology development in multiphase latex particles", *Progress in Organic Coatings*, **61**, pp. 156-165, 2008.

11. S. Shi, S. Kuroda, S. Tadaki, H. Kubota, "Phase distribution and separation in poly(2-acetoxyethyl methacrylate)/polystyrene latex interpenetrating polymer networks", *Polymer*, **43**, pp. 7443-7450, 2002.
12. P.A. Steward, J. Hearn, M.C. Wilkinson, "An overview of polymer latex film formation and properties", *Advances in Colloid and Interface Science*, **86**, pp. 195-267, 2000.
13. X. Yuan, D. Huo, Q. Qian, "Effect of annealing on the phase structure and the properties of the film formed from P(St-co-BA)/P(MMA-co-BA) composite latex", *Journal of Colloid and Interface Science*, **346**, pp. 72-78, 2010.
14. E. Arda, Ö. Pekcan, "Effect of molecular weight on packing during latex film formation", *Journal of Colloid and Interface Science*, **234**, pp. 72-78, 2001.
15. V.R. Gundabala, A.F. Routh, "Thinning of drying latex films due to surfactant", *Journal of Colloid and Interface Science*, **303**, pp. 306-314, 2006.
16. Y. Ma, H.T. Davis, L.E. Scriven, "Microstructure development in drying latex coatings", *Progress in Organic Coatings*, **52**, pp. 46-62, 2005.
17. A. T. Koshy, B. Kuriakose, and S. Thomas, "Studies on the effect of blend ratio and cure system on the degradation of natural rubber—ethylene-vinyl acetate rubber blends", *Polymer Degradation and Stability*, **36**(2), pp. 137–147, 1992.
18. A. T. Koshy, B. Kuriakose, S. Thomas, and S. Varghese, "Studies on the effect of blend ratio and crosslinking system on thermal, X-ray and dynamic mechanical properties of blends of natural rubber and ethylene-vinyl acetate copolymer", *Polymer*, **34**(16), pp. 3428–3436, 1993.
19. A. T. Koshy, B. Kuriakose, S. Thomas, and S. Varghese, "Viscoelastic properties of silica-filled natural rubber and ethylene-vinyl acetate copolymer blend", *Polymer-Plastics Technology and Engineering*, **33**(2), pp. 149–159, 1994.
20. P. Jansen, B. G. Soares, "Effect of compatibilizer and curing system on the thermal degradation of natural rubber/EVA copolymer blends", *Polymer Degradation and Stability*, **52**(1), pp. 95–99, 1996.
21. P. Jansen, A. S. Gomes, and B. G. Soares, "The use of EVA containing mercapto groups in natural rubber-EVA blends. II. The effect of curing system on mechanical and thermal properties of the blends", *J. Appl. Polym. Sci.*, **61**(4), pp. 591–598, 1996.
22. C.C. Ho, M.C. Khew, "Low glass transition temperature rubber latex film formation studied by atomic force microscopy", *Langmuir*, **16**, pp. 2436-2449, 2000.

23. Y. Wang, D. Juhué, M.A. Winnik, O.M. Leung, M.C. Goh, "Atomic force microscopy study of latex film formation", *Langmuir*, **8**, pp. 760-762, 1992.
24. C. Amornchaiyapitak, W. Taweepreda, P. Tangboriboonrat, "Modification of epoxidised natural rubber film surface by polymerisation of methyl methacrylate", *European Polymer Journal*, **4**(6), pp. 1782-1788, 2008.
25. W. Anancharungsuk, W. Taweepreda, S. Wirasate, R. Thonggoom, P. Tangboriboonrat, "Reduction of surface friction of natural rubber film coated with PMMA particle: Effect of particle size", *Journal of Applied Polymer Science*, **115**(6), pp. 3680-3686, 2010.

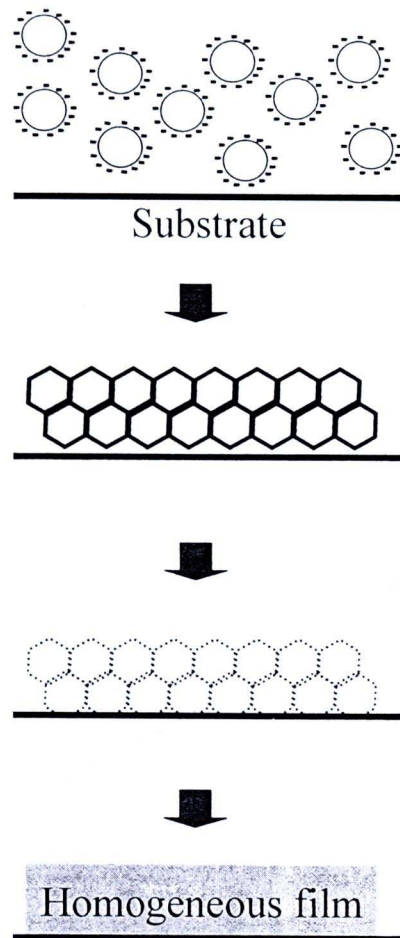


Figure 1 Film formation mechanism.

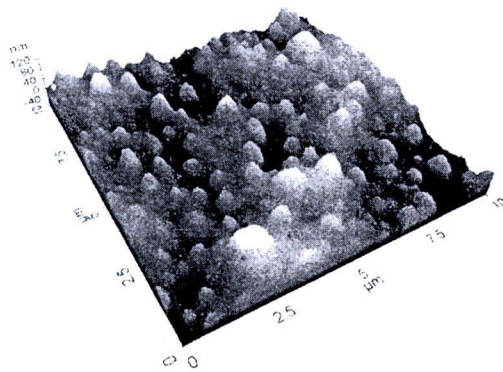


Figure 2 AFM images of NRL latex film on pre-cleaned mica surface at room temperature.



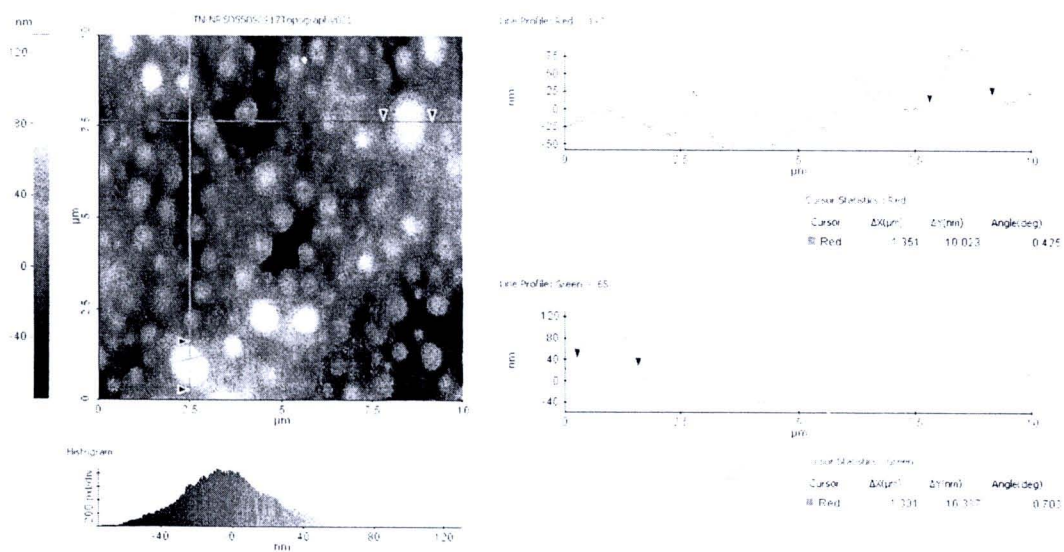


Figure 3 Measurement of NRL membrane surface roughness using AFM.

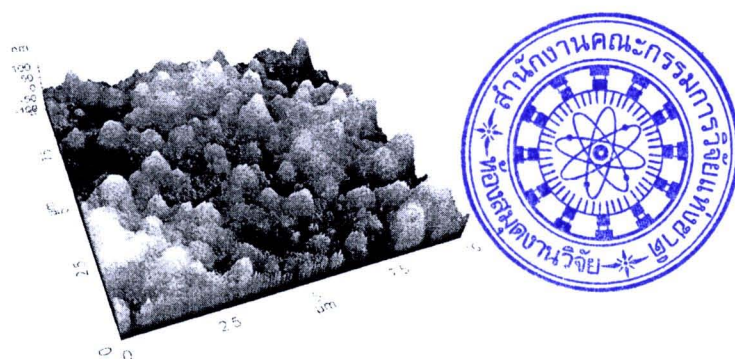


Figure 4 AFM images of XSBR latex film on pre-cleaned mica surface.

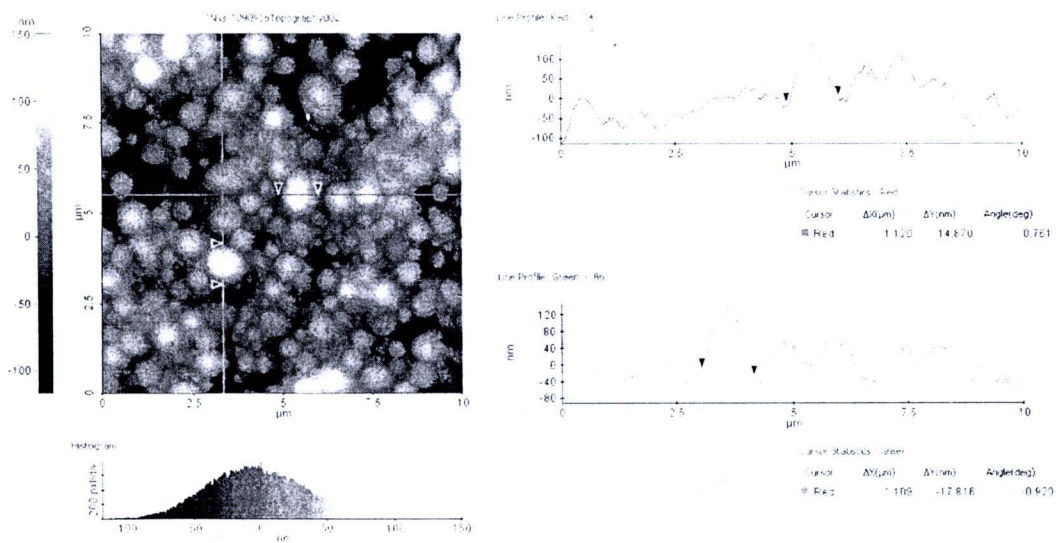


Figure 5 Measurement of XSBR film surface roughness using AFM.

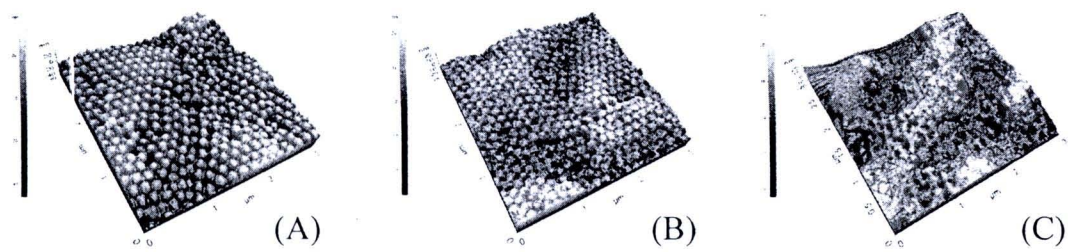


Figure 6 AFM images of XSBR film drying at:
(A) room temperature (B) 100°C and (C) 120°C.

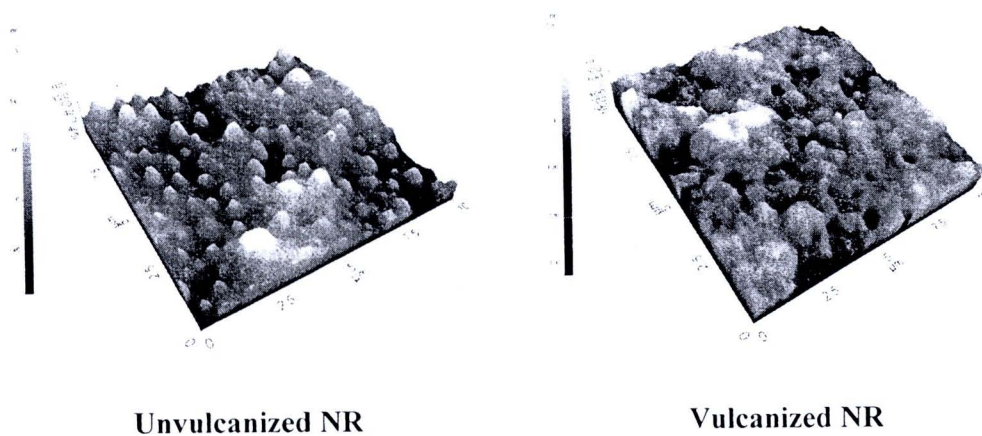


Figure 7 AFM images of NR latex compound film on mica surface.

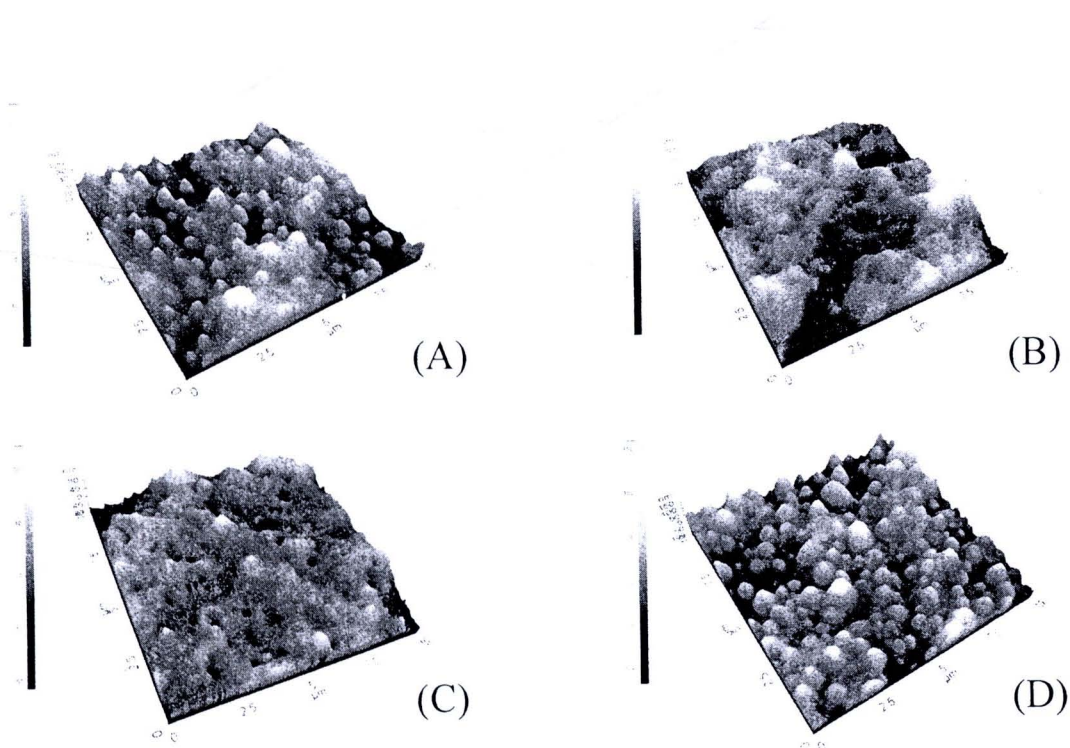


Figure 8 AFM images of drying latex film at room temperature:

(A) NR (B) XSBR 25 : NR 75 (C) XSBR 75 : NR 25 and (D) XSBR.

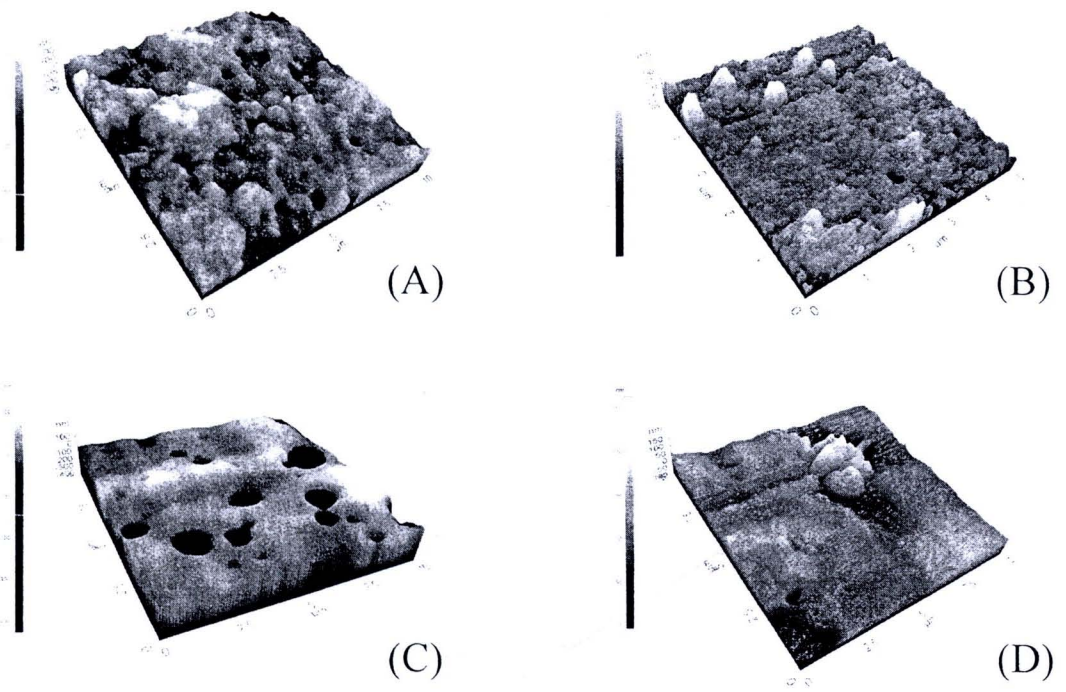


Figure 9 AFM images of vulcanized latex film at 120°C:

(A) NR (B) XSBR 25 : NR 75 (C) XSBR 75 : NR 25 and (D) XSBR.

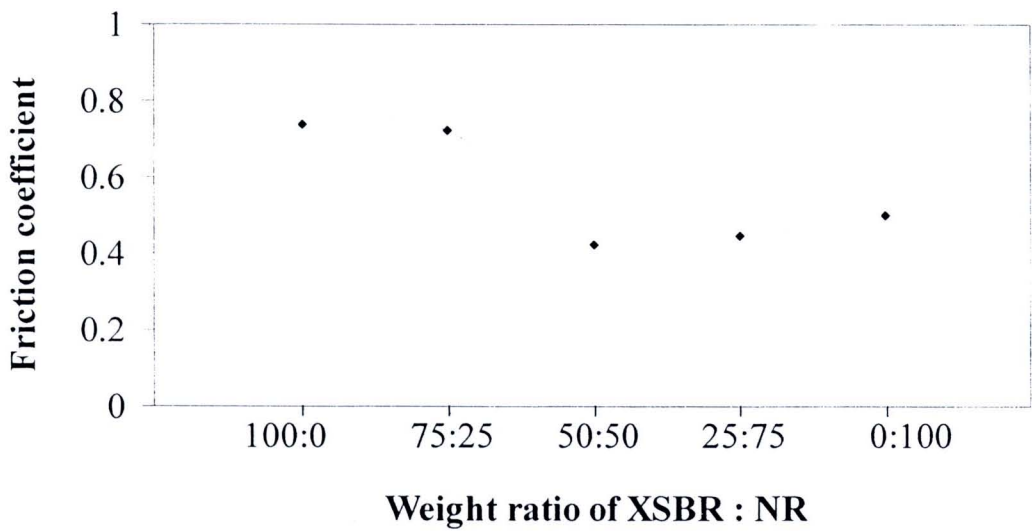


Figure 10 Friction coefficient of NR and NR/XSBR blends.

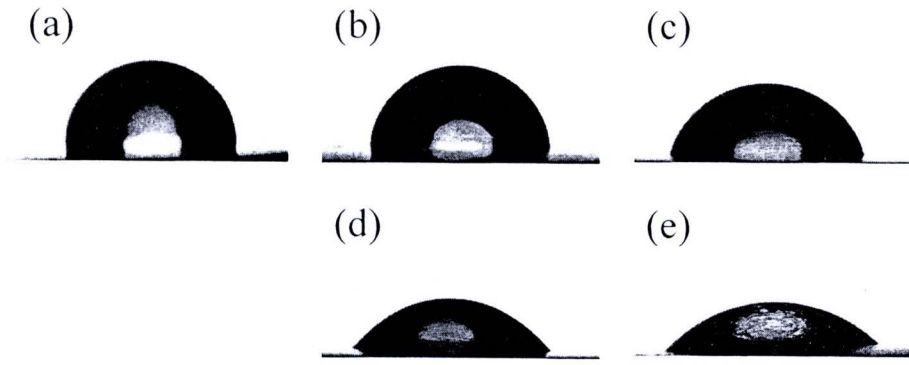


Figure 11 Water drop shape on latex membrane

(A) NR (B) XSBR 25 : NR 75 (C) XSBR 75 : NR 25 and (D) XSBR.

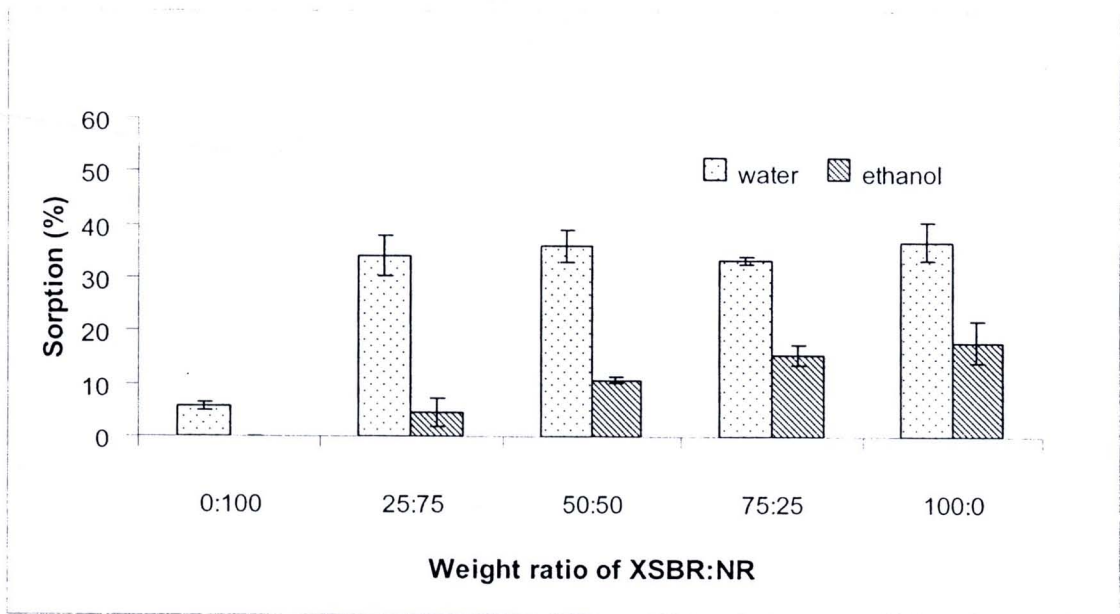


Figure 12 Water and ethanol sorption of NR and NR/XSBR blends.

Interfacial Crosslinking of Natural Rubber with Synthetic Resin Latex As Monitored by XANES

Wirach Taweepreda^{1,3*}, Rattapong Nu-Mard¹, Prayoon Songsiriritthigul², Jareon Nakason³

¹*Membrane Science and Technology Research Center, Department of Materials Science and Technology, Faculty of Science, Prince of Songkla University, Songkhla 90112, Thailand*

²*School of Physics, Suranaree University of Technology and National Synchrotron Research Center, Muang, Nakhon Ratchasima 3000, Thailand*

³*Center of Excellence in Natural Rubber Technology (CoE-NR), Department of Rubber Technology and Polymer Science, Faculty of Science and Technology, Prince of Songkla University, Pattani 94000, Thailand*

Abstract:

The sulfur crosslinking films from Natural Rubber (NR), Carboxylated Styrene Butadiene Rubber (XSBR) latices, and their blends have been investigated using X-ray absorption near-edge structure spectroscopy (XANES). The film was prepared by casting the latex compound on glass surface and heating at 120°C in a hot air oven for 10 minutes. The mechanical properties of latex blends were dramatically decreased with increasing XSBR content due to the immiscibility and sulfur crosslinking density of the blends. The immiscibility was observed using dynamic mechanical thermal analysis (DMTA) technique. The sulfur crosslinking density and oxidation states of sulfur bonding during degradation processes by thermal were studied by the XANES. This was done to provide the local geometry and electronic environment of sulfur bonding in the rubber networks. We found that the reversion takes place before the onset of oxidative processes at the sulfur bridges. Parallel to the oxidative processes, the production of cyclic sulfanes takes places. This relationship depends on the rubber compositions.

Keywords: rubber, latex, latex blend, sulfur crosslinks, XANES

*Corresponding author. Tel.: +66-67-785004; Fax: +66-74-446925
E-mail address: wirach.t@psu.ac.th

1. Introduction

Natural rubber (NR) has excellent mechanical properties and heat build-up but poor thermal oxidation resistance due to it contains double bonds in the molecular structure [1-2]. The blending of NR with synthetic rubbers such as styrene-butadiene rubber (SBR), carboxylated styrene-butadiene rubber (XSBR), butadiene rubber (BR), and acrylonitrile butadiene rubber (NBR) have been tried to obtain desirable properties [3]. The properties of rubber such as tensile strength, elongation at break, oil, and thermal resistance, etc. exhibit after introducing crosslink to rubber in a vulcanization process. Blends of NR have been reported to be compatible with desirable mechanical properties [4-8]. However, the blending of NR with some polar synthetic rubber is difficult task to obtain the desirable properties due to their incompatible nature and hence, they tend to separate out. Furthermore, it is the relative crosslink densities within the individual rubber phase which is of concern and not the extent of crosslinking between the two, although this is also of considerable importance to properties. Thus, better understanding of the vulcanization in a molecular scale is necessary. Sulfur vulcanization is a chemical reaction between rubber and vulcanizing agents and commonly used to crosslink the NR to fabricate many of NR products such as tire, glove and rubber thread, etc. There have been numerous attempts to understand the mechanism of sulfur vulcanization [9-16] but the sulfur vulcanization of NR is still complicated. Recently, the simple model compounds with molecular structure similar to NR have been studied to clarify the sulfur vulcanization process using X-ray absorption near-edge spectroscopy (XANES). [17] It was found that vulcanization with different accelerator yield vary in crosslink bonding length. XANES technique is also used to explain the processes occurring at the sulfur crosslinks of vulcanized rubber during thermo-oxidative aging. [18-19] It should be recognized that sufficient crosslinking between two rubbers in a blend will be less likely if one component is poorly crosslinked at the end of the vulcanization process. Even though, there are many well-established techniques have been applied to characterize the crosslink distributions in rubber blends: dynamic mechanical thermal analysis (DMTA) [20-21], differential scanning calorimetry (DSC) [22], positron annihilation lifetime spectroscopy (PALS) [23], ultrasonic measurement [24], and swollen- state NMR spectroscopy [25] but there are no report for estimating the crosslinking across the interface between the rubber blend.

In the present study, the crosslinking characteristic in NR, XSBR, and their blends are monitored using XANES according to immiscibility as well as the mechanical properties with

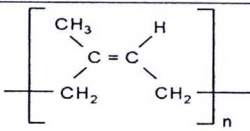
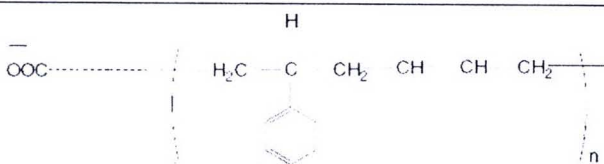
blend ratio and its effects on thermal resistance properties will be investigated, and the resulting degradation of sulfur bonding will be studied accordingly

2. Experimental

2.1 Materials

High ammonia concentrated natural rubber latex (NRL) was purchased from Chalong Concentrate Latex Industry Co., LTD. Carboxylated styrene butadiene copolymer latex (XSBR) was supplied by Synthomer GmbH. Chemical structure and properties of the latex are illustrated in table 1. The rubber chemicals for example zinc oxide (ZnO), sulfur (S₈), zinc diethyldithiocarbamate (ZDEC), and vulcanox CPL were all obtained from Lucky four (Bangkok, Thailand) and used without further purification.

Table 1 Characteristic of latex.

NRL		
Dry rubber contents (%DRC)	60.14	
Total solid content (%TSC)	61.68	
pH	10.51	
Glass transition temperature (°C)	-68	
Specific gravity @25°C	0.92	
XSBR (SYNTHOMER 79Q10)		
Total solid content (%TSC)	50.0	
pH	5.7	
Glass transition temperature (°C)	+4	
Specific gravity @25°C	1.02	

2.2 Preparation of samples

NR and XSBR latex were readily mixed together for 10 minutes at an ambient temperature with the following blending ratios: 75:25, 50:50, and 25:75 w/w; based on dry rubber content. For compounding were mixed with chemicals followed Table 2 with mechanical stirred for 24 hours and matured 24 hours at an ambient temperature. The latex films were formed by

casting with casting knife on the glass plate with thickness not over than 0.2 mm, approximately. Then, the natural rubber latex films were dried at room temperature and vulcanization was finally at 120°C for 10 minute.

Table 2 Formulation of latex compound.

Compositions	Part per hundred of rubber (phr)				
	1	2	3	4	5
NR latex	100	57	50	25	0
XSBR latex	0	25	50	75	100
KOH 10% solution	0.5	0.5	0.5	0.5	0.5
K'oleate 10% solution	0.25	0.25	0.25	0.25	0.25
Sulfur 50% dispersion	1.0	1.0	1.0	1.0	1.0
Zinc oxide 50% dispersion	0.5	0.5	0.5	0.5	0.5
ZBDC 50% dispersion	1.0	1.0	1.0	1.0	1.0
Vulcanox CPL50% dispersion	0.75	0.75	0.75	0.75	0.75

2.3 Measurements

2.3.1 Tensile strength measurement

The tensile strength measurements were done in a Tensile Testing Machine (LLOYD Instruments Series 10K) according to ASTM D638M at a strain rate of 100 mm/min. Five specimens were used for each measurement and the median value was used as the tensile strength. The error bar given in the figures reported in this work was the upper and lower limit of tensile strength values of specimens. The aged samples in the oven at 70°C for 7 days were measured and compared.

2.3.2 Dynamic Mechanical Thermal Analysis

The dynamic mechanical properties of NR and NR/XSBR blends were performed using Dynamic Mechanical Thermal Analyser (DMTA; Model-V, supplied by Rheometric Scientific). The shape of test sample was rectangular, 25 mm long, 10 mm wide and 1.5 mm thick. The single cantilever mode of deformation was used under the test temperature range from -100°C to 70°C with a heating rate of 3°C/min.; the test frequency being 1 Hz. The cooling process was achieved through liquid nitrogen. The results were presented in terms of loss tangent ($\tan\delta$) and glass transition temperature (T_g). In this work, loss tangent ($\tan\delta$) was

the ratio of loss modulus (E'') to storage modulus (E') whereas T_g was obtained from the loss modulus peak.

2.3.3 X-ray absorption spectroscopy (XAS)

XANES measurements were carried out at beamline 8 of the Synchrotron Light Research Institute (SLRI) in Thailand [24]. The energy scan was carried out using the Si(111) double crystal monochromator to cover the K -edge of sulfur. The white line of zinc sulfate ($ZnSO_4$) powder was used as the reference energy of 2481.4 ± 0.1 eV [25]. The reproducibility of this energy in our measurements is better than 0.07 eV. The step width of the energy scan used for in this work is 0.1 eV. For the vulcanized rubber sheet of all sample sets was cut and placed on a 12 mm x 6 mm sample holder. The photon beam size was 10 mm x 1 mm. All XAS spectra around the K -edge of sulfur were recorded using two ionization chambers. They were filled with air at 60 mbar and located before and after the sample to record the incoming and transmitted photon beam intensity. All of the XANES spectra were averaged and normalized using IFEFFIT software, version 1.2.11.

3. RESULTS AND DISCUSSION

3.1 Mechanical properties

The tensile strength of NR film is higher than the tensile strength of XSBR film because of the crystallization of NR. Blending of NR with XSBR latex decreased the tensile strength and elongation at break of latex film while the 300% modulus was increased as shown in figure 1. The results indicated that molecular weight of cross-linking (M_c) of XSBR film should be higher than that of NR as illustrated in figure 2. In the same way, the cross-linking density of NR is higher than that of XSBR film. XSBR latex consisted with double bond less than NR so the properties of thin film after thermal aging are improved in NR/XSBR blend films.

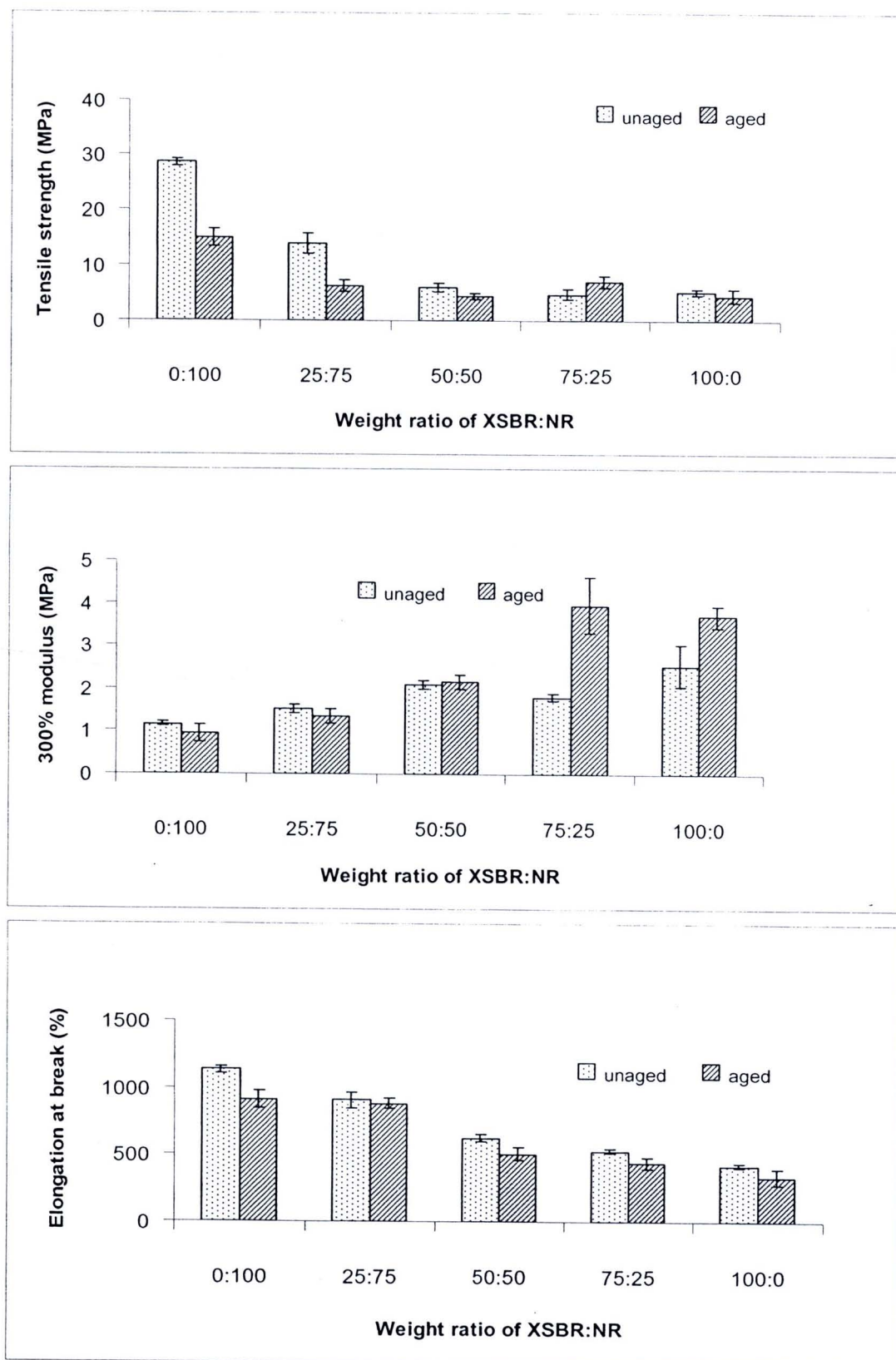


Figure 1 Mechanical property of vulcanized latex films for different blend ratios.

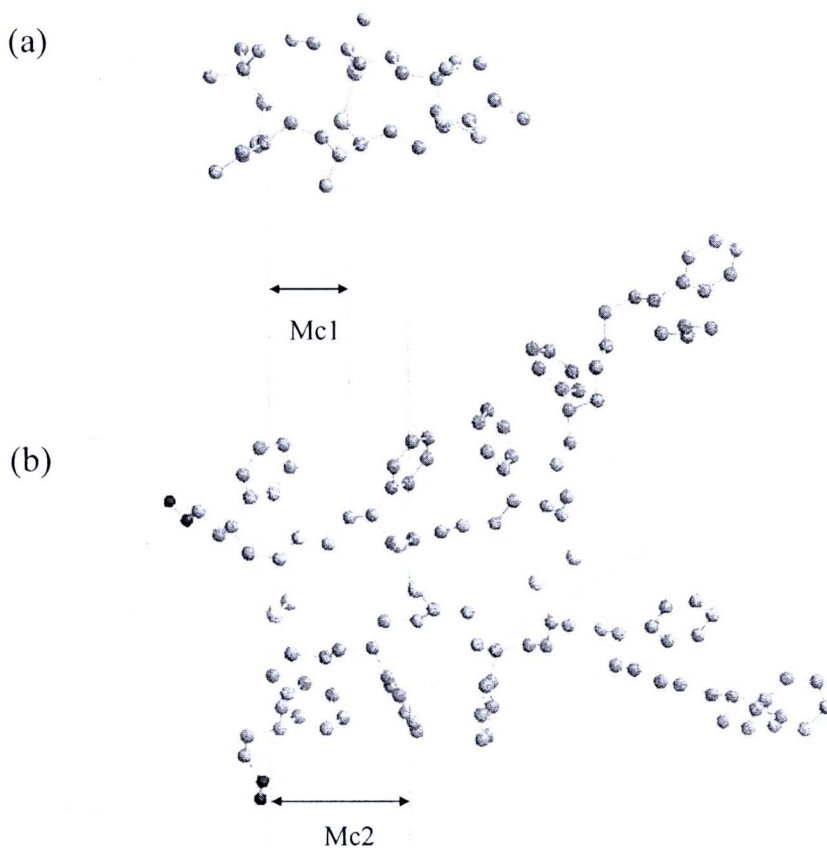


Figure 2 Molecular modeling of sulfidic crosslinked in (a) NR and (b) XSBR.

3.2 Dynamic Mechanical Thermal Analysis

Glass transition temperature of NR and NR/XSBR blend films were investigated by dynamical mechanical analysis. In figure 3 and 4, $\tan \delta$ of NR and NR/XSBR blend films show a maximum at temperature between -51.4°C and 20.1°C that can be attributed to the glass transition temperature, T_g . T_g of the NR vulcanizates is increased with increasing sulfur concentration as shown in figure 3. For less efficient sulfur cure systems (S:ZBDC 5:1), no crystallization was observed [22], imposed restrictions on molecular mobility due to crosslink density increases and increasing main chain modifications. For the NR/XSBR blend, T_g is shifted arising from vulcanization as shown in figure 4. The T_g of NR/XSBR blend film shows two values at -41.1°C and 20.1°C for NR and XSBR phase, respectively. The shifting peak of NR and XSBR phase in NR/XSBR blend corresponding to the minority phase in the NR/XSBR blend as demonstrated in figure 5. XSBR is readily vulcanized by not only sulfur but also ZnO owing to the presence of carboxyl groups as a result of formation of a tridimensional structure caused by the orientation effect [26]. In the presence of ZnO, the

XSBR are vulcanized by the formation of salt-like bonds combined with sulfidic bonds and the participation of the carboxyl groups attached to different chains results in carbon-carbon bonds [27]. The blending of NR with XSBR will enhance the physical and mechanical properties of the vulcanizate and the rubber is highly resistant to thermal aging.

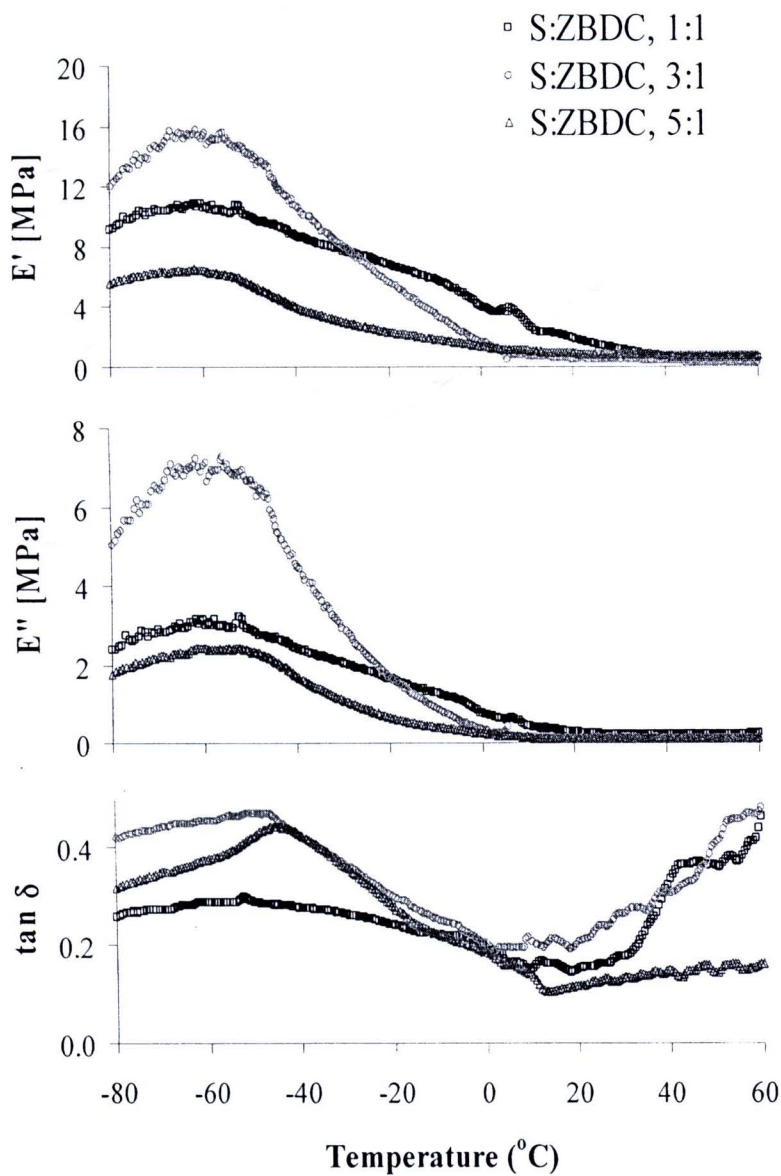


Figure 3 Storage modulus (E'), loss modulus (E'') and loss factor ($\tan \delta$) versus temperature of vulcanized NR for different sulfur concentration.

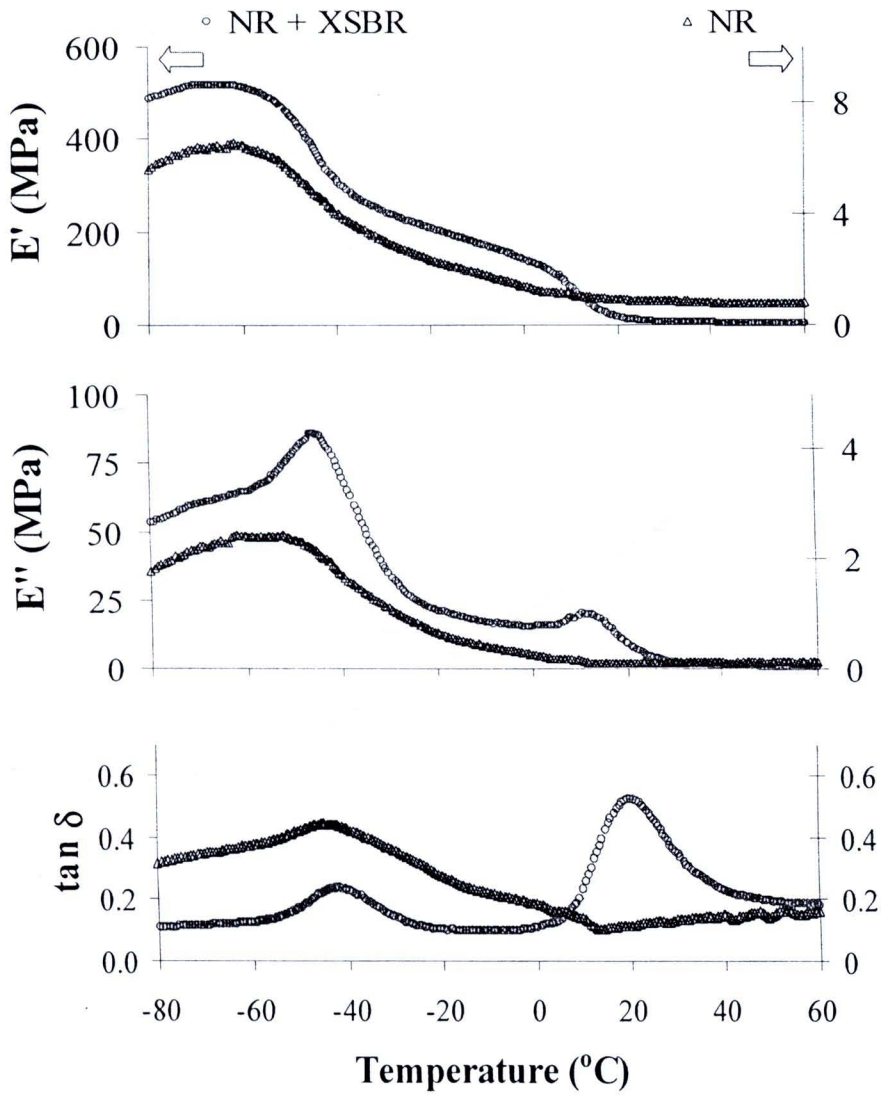


Figure 4 Storage modulus (E'), loss modulus (E'') and loss factor ($\tan \delta$) versus temperature of vulcanized NR and NR/XSBR blend films.



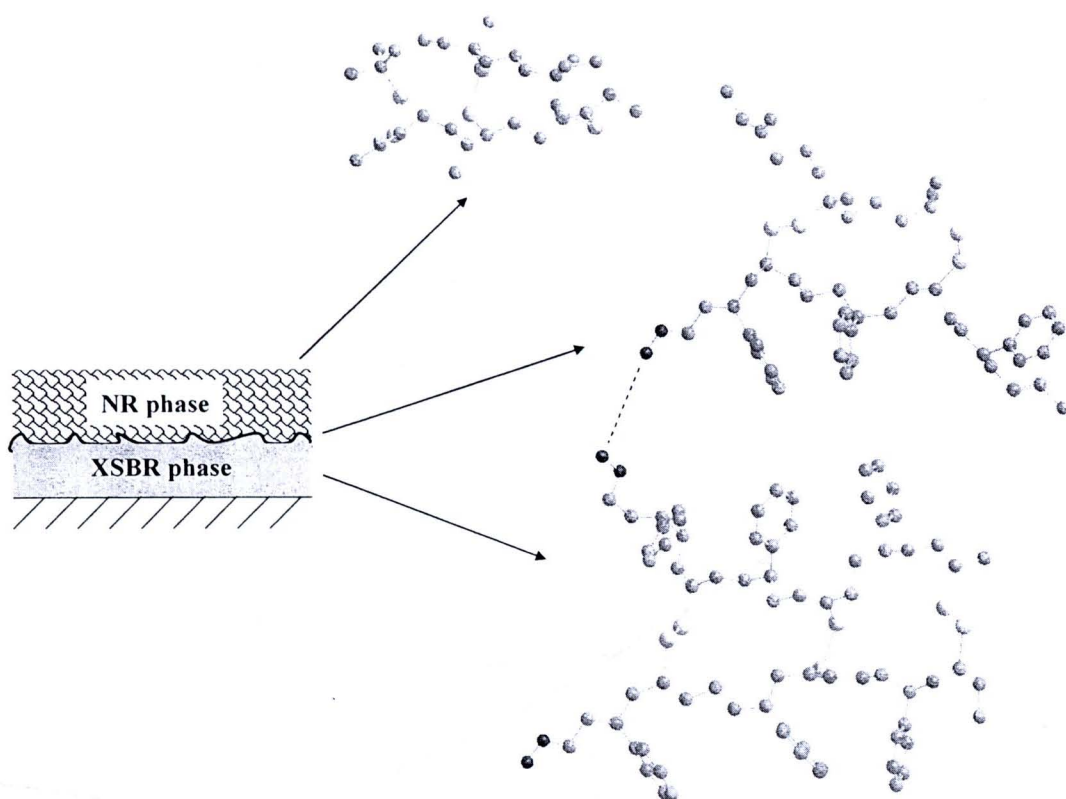


Figure 5 Molecular modeling of sulfur crosslink NR/XSBR blend film.

3.3 X-ray absorption near edge structure spectroscopy (XANES)

The sulfur crosslink bonding in rubber molecule was characterized using X-ray absorption near edge structure spectroscopy (XANES) has been established [18-19]. The S K-edge absorption peak, cover photon energy range of 2465-2490 eV with the accuracy of photon energy up to within 0.2 eV, would shift depending on sulfur environment. Figure 6 shows the XANES spectra of the vulcanized NR. Vulcanized NR with S:ZBDC at the ratio 2:2 show absorption peak lower than that with less efficient sulfur cure systems (S:ZBDC 5:2). These peaks correspond to the electronic transitions of $\sigma^*(\text{S-C resonance})$ and $\sigma^*(\text{S-C resonance})$ bonds formed after vulcanization [8]. The assignment of the σ^* resonance peaks referred to in this work are based on the reports of Hitchcock [30], Sze [31] and George [32]. There has also been reports that the absorption peak shifts towards higher photon energy when the number of sulfurs in $\text{C-S}_x\text{-C}$ ($x=1,2,3,4$) chains decreases [33-34]. The higher photon energy of the peak at 2472.5 eV in the XANES spectra of less efficient sulfur cure system (S:ZBDC 5:2) indicates that the majority of the crosslink may be disulfidic whilst semi-efficient vulcanization (S:ZBDC 2:2) shows lower photon energy peak at 2471.5 eV

indicates yield polysulfidic crosslink in NR vulcanizate. It is interesting to point out from the measured XANES spectra that the effects of sulfur cure system on the crosslink bond type are correlated with dynamic mechanical properties of NR vulcanizates in molecular scale.

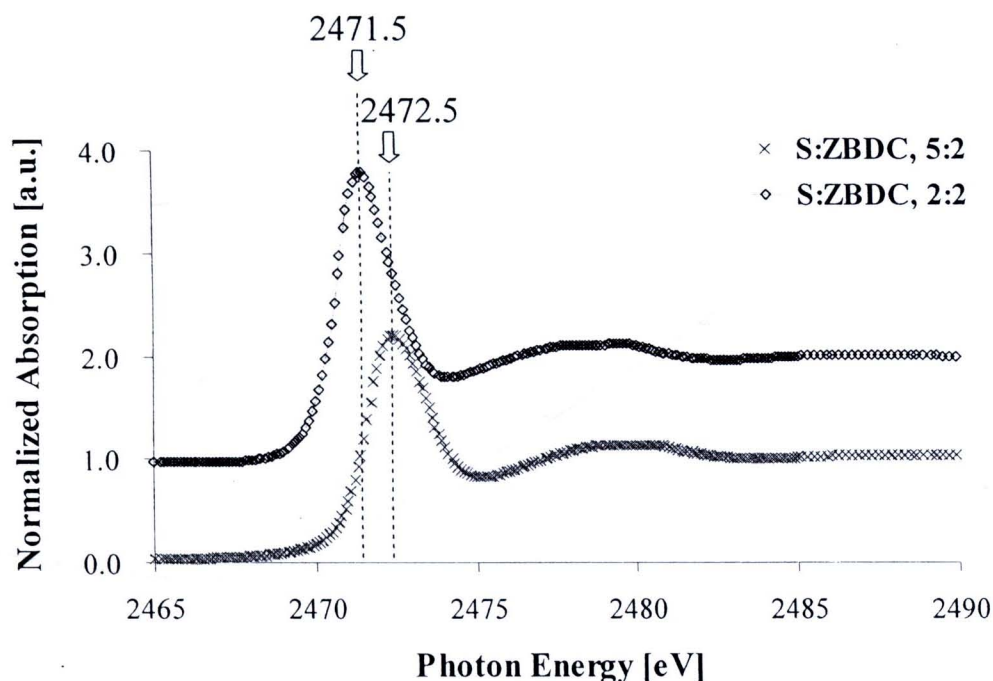


Figure 6 S K-edge XANES spectra of vulcanized NR for different vulcanization system.

The formation of sulfide cross-linking in XSBR film is less than in NR film. The S K-edge absorption at 2481.4 eV in XSBR film indicated the amount of free sulfur which is not reacted to form the linkage. This evidence is strongly supported the mechanical properties of XSBR film that it is weaker than the NR film. The blending of NR with XSBR, high T_g XSBR particle might be separated and transferred to the other layer of the latex film from soft NR particles. Moreover, the double bond of XSBR particles is less than that of NR particles. The crosslinking density of latex blend film is decreased with increasing the XSBR particles as illustrated in figure 7. Figure 8 shows the effect of sulfur concentration on sulfidic bonding type, found that the absorption peaks are very similar.

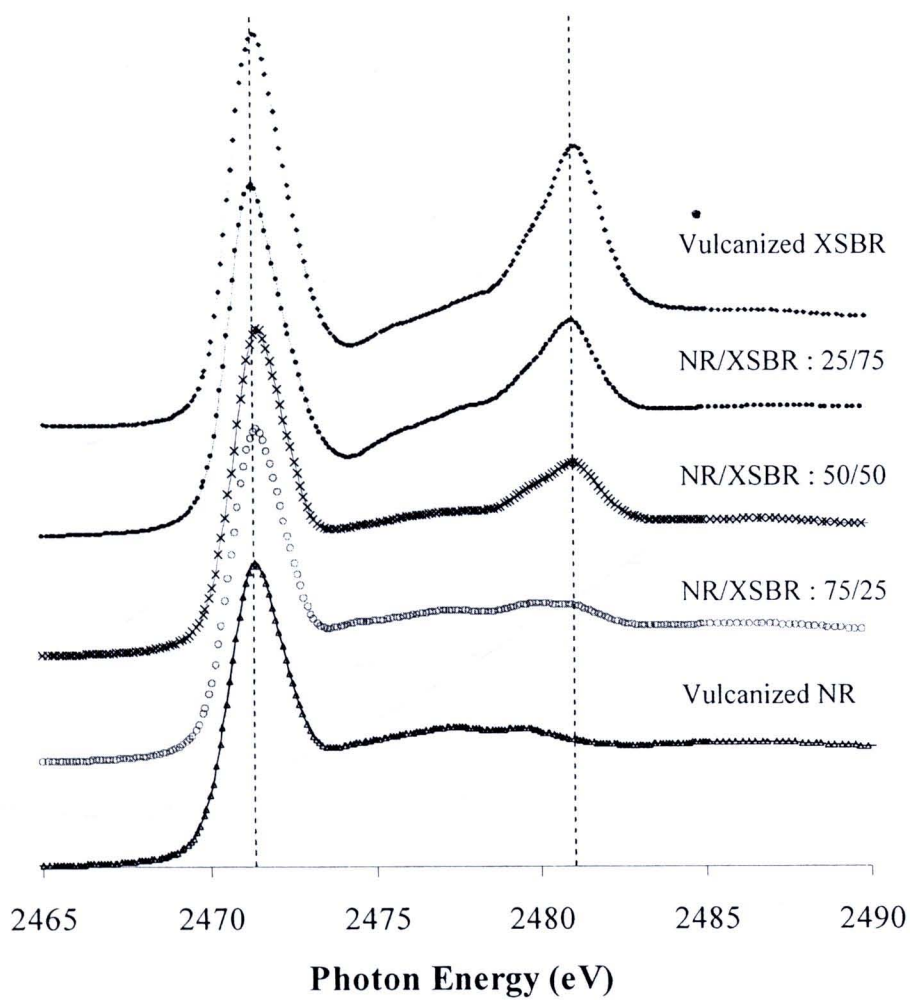


Figure 7 S K-edge XANES spectra of NR/XSBR latex film for different blend ratios.

Compositions	phr	phr
NR latex	75	75
XSBR latex	25	25
KOH 10%	0.2	0.2
K'oleate 10%	0.25	0.25
Sulphur 50%	1	3
Zinc oxide 50%	0.5	0.5
ZBDC 50%	1	1
Vulcanox CPL 50%	0.75	0.75

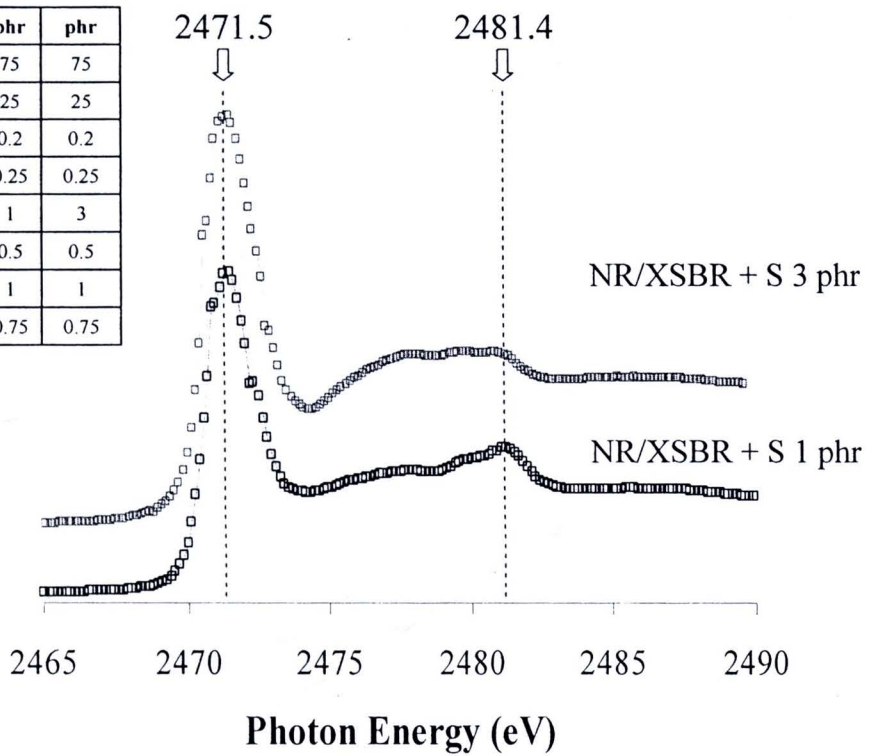


Figure 8 S K-edge XANES spectra of NR/XSBR latex film for different sulfur concentration.

4. Conclusion

In conclusion, NR is immiscible blend with XSBR latex due to the polarity of XSBR particles. The immiscibility of the latex blends is indicated by DMTA results. The NR/XSBR thermogram appears two T_g value of NR phase at -51.4°C and XSBR phase at $+20.1^{\circ}\text{C}$. The T_g of XSBR increases from $+4^{\circ}\text{C}$ to $+20.1^{\circ}\text{C}$ after blending with NR. The hard XSBR particles seem to transfer to the top of film layer and form boundary layer. The mechanical properties of film formed from NRL particle is poor after blending with hard XSBR particle due to the crosslinking characteristic and density. XANES technique is the direct method for characterization of sulfic crosslink in latex film. The free sulfur in latex blend film is increased with increasing the XSBR concentration due to double bond in XSBR molecular structure is less than that of NR. On the other hand, the molecular weight of crosslinking of XSBR is high. Moreover, XANES results can specify the sulfidic bonding type and found that it is correlated with mechanical properties of latex blend film.

Acknowledgement

W.T. would like to thank the Thailand Research Fund (TRF)/the Commission on Higher Education (CHE) as the research grant (contact reference number MRG5080206). One of the authors (R.N.) would like to thank SLRI for a scholarship (contract number 2550/03-GS-50-M03).

References

- [1] Md. S. Nordin, "Synergistic combinations of antioxidants for natural rubber vulcanisates", *J. Rubb. Res. Inst. Malaysia*, **26**(2), pp. 79-84, 1978.
- [2] M. Chen, N. -J. Ao, Y. Chen, J. -L. Qu, H. -P. Y., C. Wang, H. -L. Zhou, H. -L. Qian, "Effect of an antioxidant system on the structure and properties of natural rubber-clay composite", *J. Rubb. Res.*, **6**(3), pp. 164-171, 2003.
- [3] A. J. Tinker, "Distribution of Crosslinks in Vulcanized Blends", *Rubber Chem. Technol.*, **68**, pp. 461-480, 1995.
- [4] A. T. Koshy, B. Kuriakose, and S. Thomas, "Studies on the effect of blend ratio and cure system on the degradation of natural rubber—ethylene-vinyl acetate rubber blends", *Polymer Degradation and Stability*, **36**(2), pp. 137–147, 1992.
- [5] A. T. Koshy, B. Kuriakose, S. Thomas, and S. Varghese, "Studies on the effect of blend ratio and crosslinking system on thermal, X-ray and dynamic mechanical properties of blends of natural rubber and ethylene-vinyl acetate copolymer", *Polymer*, **34**(16), pp. 3428–3436, 1993.
- [6] A. T. Koshy, B. Kuriakose, S. Thomas, and S. Varghese, "Viscoelastic properties of silica-filled natural rubber and ethylene-vinyl acetate copolymer blend", *Polymer-Plastics Technology and Engineering*, **33**(2), pp. 149–159, 1994.
- [7] P. Jansen, B. G. Soares, "Effect of compatibilizer and curing system on the thermal degradation of natural rubber/EVA copolymer blends", *Polymer Degradation and Stability*, **52**(1), pp. 95–99, 1996.
- [8] P. Jansen, A. S. Gomes, and B. G. Soares, "The use of EVA containing mercapto groups in natural rubber-EVA blends. II. The effect of curing system on mechanical and thermal properties of the blends", *J. Appl. Polym. Sci.*, **61**(4), pp. 591–598, 1996.
- [9] B. Saville, A. A. Watson, "Structural characterization of sulfur-vulcanized rubber networks", *Rubber Chem. Technol.*, **40**, pp. 100-148, 1967.

- [10] T. D. Skinner, "The CBS-accelerated sulfuration of natural rubber and cis-1,4-polybutadiene", *Rubber Chem. Technol.*, **45**, pp. 182-192, 1972.
- [11] M. R. Krejsa, J. L. Koeing, "A review of sulfur crosslinking fundamentals for accelerated and unaccelerated vulcanization", *Rubber Chem. Technol.*, **66**, pp. 376-410, 1993.
- [12] P. J. Nieuwenhuizen, J. Reedijk, "Thiuram- and dithiocarbamate-accelerated sulfur vulcanization from the chemist's perspective; methods, materials and mechanisms reviewed", *Rubber Chem. Technol.*, **70**, pp. 368-429, 1997.
- [13] P. Ghosh, S. Katare, P. Patkar, J. M. Caruthers, V. Venkatasubramanian, "Sulfur vulcanization of natural rubber for benzothiazole accelerated formulations: from reaction mechanisms to a rational kinetic model", *Rubber Chem. Technol.*, **76**, pp. 592-693, 2003.
- [14] G. Heideman, R. N. Datta, J. W. M. Noordermeer, "Activators in accelerated sulfur vulcanization", *Rubber Chem. Technol.*, **77**, pp. 512-541, 2004.
- [15] A. Y. Coran, "Chemistry of the vulcanization and protection of elastomers: A review of the achievements", *J. Appl. Polym. Sci.*, **87**, pp. 24-30, 2003.
- [16] W. Choi, "The main mechanism and cross-linking structure for accelerated sulfur vulcanization", *e-J. Soft Mater.*, **2**, pp. 47-55, 2006.
- [17] W. Taweepreda, R. Nu-Mard, W. Pattanasiriwisawa, P. Songsiriritthigul, "Model Compound Vulcanization Studied by XANES", *J. Phys.: Conf. Ser.*, **190**, 012150, 2009.
- [18] H. Modrow, J. Hormes, F. Visel, R. Zimmer, "Monitoring thermal oxidation of sulfur crosslinks in SBR-elastomers by quantitative analysis of sulfur K-edge XANES-spectra", *Rubber Chem. Technol.*, **74**, pp. 281-294, 2001.
- [19] H. Modrow, R. Zimmer, F. Visel, J. Hormes, "Monitoring thermal oxidation of sulfur crosslinks in SBR-elastomers using sulfur K-edge XANES: A feasibility study", *Kautsch. Gummi Kunstst.*, **53**, pp. 328-337, 2000.
- [20] S. H. Mansour, S. Y., Tawfik, M.H., Youssef, "Unsaturated polyester resin as compatibilizer for SBR/NBR rubber blends", *J. Appl. Polym. Sci.*, **83**, pp. 2314-2321, 2002.
- [21] M. H., Youssef, "Temperature dependence of the degree of compatibility in SBR-NBR blends by ultrasonic attenuation measurements: influence of unsaturated polyester additive", *Polymer*, **42**, pp. 10055-10062, 2001.
- [22] S. Cook, S. Groves, A.J. Tinker, "Investigating crosslinking in blends by differential scanning calorimetry", *J. Rubb. Res.*, **6**(3), pp. 121-128, 2003.
- [23] W. Salgueiro, A. Somozaa, A.J. Marzocca, G. Consolati, F. Quasso, "Evolution of the crosslink structure in the elastomers NR and SBR", *Radiation Physics and Chemistry*, **76**, pp. 142-145, 2007.

- [24] W. Klysubun, P. Sombunchoo, N. Wongprachanukul, P. Tarawarakarn, S. Klinkhico, J. Chaiprapa, P. Songsiriritthigul, "Commissioning and performance of X-ray absorption spectroscopy beamline at the Siam Photon Laboratory", *Nucl.Instrum. Methods Phys. Res.*, **582** pp. 87–89, 2007.
- [25] B. Ravel, M. Newville, "ATHENA, ARTEMIS, HEPHAESTUS: data analysis for X-ray absorption spectroscopy using IFEFFIT", *J. Synchrotron Rad.*, **12** pp. 537–541, 2005.
- [26] B. Dolgoplosk, E.T. Akova, V. Reikh, *Kauchuk I Rezina*, No.3:11, 1957.
- [27] G.A. Blokh, *Organic Accelerators in the Vulcanization of Rubber* (Israel Program for Scientific Translations Ltd., Jerusalem, 1968) pp. 99-102.
- [30] A.P. Hitchcock, S. Bodeur, M. Tronc, *Chem. Phys.*, **115** pp. 93-101, 1987.
- [31] K.H. Sze, C.E. Brion, M. Tronc, S. Bodeur, A.P. Hitchcock, *Chem. Phys.* **121** pp. 279-297, 1988.
- [32] G.N. George, M.L. Gorbaty, *J. Am. Chem. Soc.* **111** pp. 3182-3186, 1989.
- [33] R. Chauvistré, J. Hormes, E. Hartmann, N. Etzenbach, R. Hosch, J. Hahn, *Chem. Phys.* **223** pp. 293-302, 1997.
- [34] J. Hormes, M. Modrow, *Nucl Instrum Meth. A* : **467-468** pp. 1179-1191, 2001.



